ACS APPLIED MATERIALS & INTERFACES

Research Article

www.acsami.org

Cellular Membrane Enrichment of Self-Assembling D-Peptides for Cell Surface Engineering

Huaimin Wang,[†] Youzhi Wang,[†] Aitian Han,[†] Yanbin Cai,[†] Nannan Xiao,[†] Ling Wang,[‡] Dan Ding,[†] and Zhimou Yang*[,†,‡]

[†]State Key Laboratory of Medicinal Chemical Biology, Key Laboratory of Bioactive Materials, Ministry of Education, College of Life Sciences, and Collaborative Innovation Center of Chemical Science and Engineering (Tianjin), [‡]College of Pharmacy and Tianjin Key Laboratory of Molecular Drug Research, Nankai University, Tianjin 300071, People's Republic of China

Supporting Information

ABSTRACT: We occasionally found that several self-assembling peptides containing D-amino acids would be preferentially enriched in cellular membranes at self-assembled stages while distributed evenly in the cytoplasma of cells at unassembled stages. Self-assembling peptides containing only L-amino acids distributed evenly in cytoplasma of cells at both self-assembled and unassembled stages. The self-assembling peptides containing D-amino acids could therefore be applied for engineering cell surface with peptides. More importantly, by integrating a protein binding peptide (a PDZ domain binding hexapeptide of WRESAI) with the self-assembling peptide containing D-amino acids, protein could also be introduced to the cell surface. This study not only provided a novel approach to engineer cell surface, but also highlighted the unusual properties and potential applications of self-assembling peptides containing D-amino acids in regenerative medicine, drug delivery, and tissue engineering.

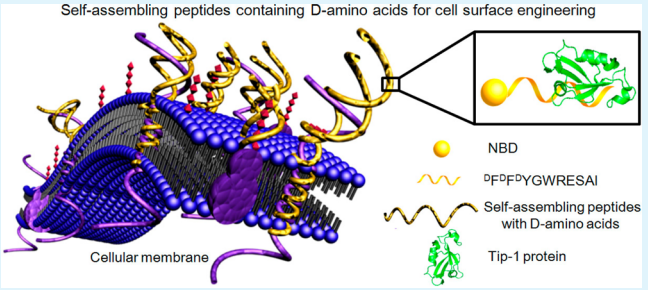

KEYWORDS: *self-assembly, nanofiber, D-peptide, cell surface engineering, cell therapy*

INTRODUCTION

Self-assembling peptide-based materials have attracted intensive research interests due to their good biocompatibility and bioactivity, as well as their ease of design and synthesis.[1−10] They have been widely used for three-dimensional (3D) cell culture,[11−13] drug delivery,[14−19] analyte detection,[20−26] cancer cell inhibition,[27−29] and regenerative medicine.[30−32] Commonly, self-assembling peptide-based materials are made of L-amino acids because nature only employs L-amino acids to synthesize proteins in the human body. Recently, results indicate that self-assembling D-peptides can possess unusual properties over their L counterparts. The D-peptides can possess improved in vivo stability due to the lack of digestion enzymes to D-peptides in human. For instance, Xu and Zhang groups have verified that the self-assembling nanofibers from D-peptides can be resistant to the digestion of proteases.[33−35] Besides, self-assembling materials consisting of D-amino acids can improve the selectivity of therapeutic agents to their targets. For example, Xu and co-workers found that the integration of D-amino acids with a nonsteroid anti-inflammatory drug (NSAID) can boost the selectivity of the NSAID to cyclooxygenase-2 (COX-2) over COX-1.[36] These pioneering works highlight the unusual properties of D-peptides and offer a novel strategy to design self-assembling peptide-based materials with unusual bioactivities.

Recent studies also showed that self-assembling peptides would interact with proteins or protein assemblies in cells and could be selectively formed in certain cells, thus providing novel strategies to manipulate the fate of cells.[37−40] These studies will also stimulate the research efforts to develop novel self-assembling materials to achieve biological functions. On the basis of these pioneering works, we opted to develop self-assembling peptides with L- and D-amino acids and studied their biological functions in cells. In this study, we occasionally find that the utilization of D-amino acids in self-assembling peptides will boost their cellular membrane localization. Although the direct reasons for such observations remain elusive, these discoveries can render many immediate applications, such as cell surface engineering.

RESULTS AND DISCUSSION

In our initial design, we planned to image actin in cells by using NBD-FFYGLKKTETQ (Scheme 1) because of the following reasons: (1) many peptides with FF or FFY possessed excellent self-assembly properties;[4,11,41,42] (2) 4-nitro-2,1,3-benzoxadiazole (NBD) was an environment-sensitive fluorophore[26,43] and had been used by us as an aromatic capping group to generate self-assembling peptides;[44] and (3) the peptide of LKKTETQ was an actin-binding domain of thymosin β-4 and β-10.[45] Therefore, NBD-FFYGLKKTETQ might self-assemble into

Received: April 14, 2014
Accepted: June 4, 2014
Published: June 4, 2014

   dx.doi.org/10.1021/am502250r | ACS Appl. Mater. Interfaces 2014, 6, 9815−9821

Scheme 1. Chemical Structures of NBD-FFYLKKTETQ, NBD-^{D}F^{D}F^{D}YLKKTETQ, and NBD-^{D}F^{D}F^{D}YG^{D}L^{D}K^{D}K^{D}T^{D}E^{D}T^{D}Q

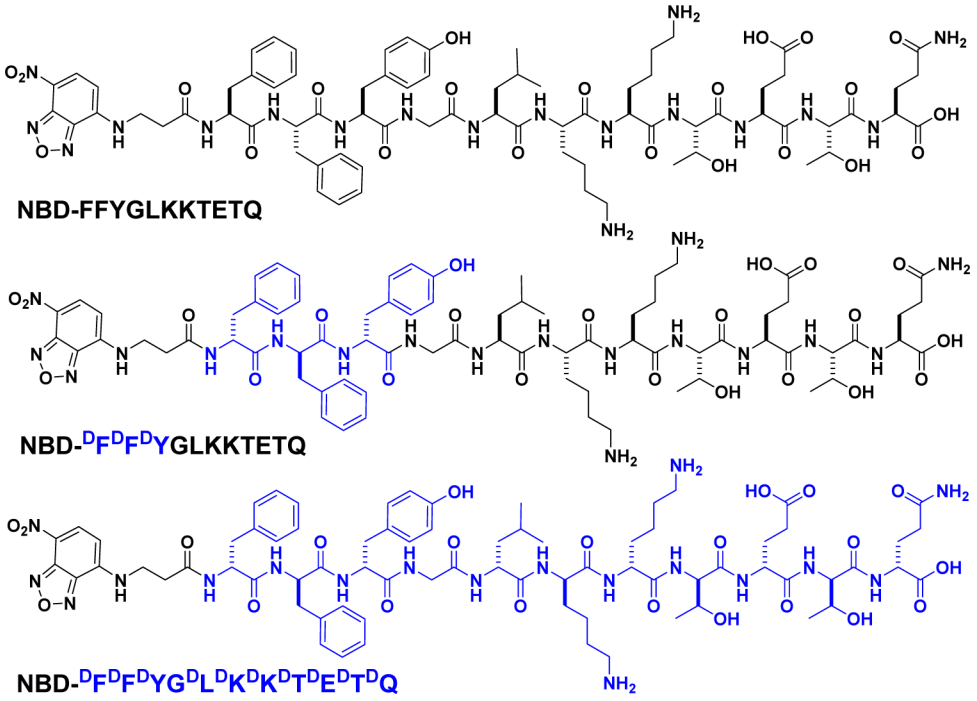

nanostructures that could bind to actin, resulting in the perturbation of the dynamic of actin. To improve the stability of the peptide in biological environments, we also designed and synthesized the peptide of NBD-^{D}F^{D}F^{D}YGLKKTETQ (Scheme 1) containing D-amino acids.

The two peptides NBD-FFYGLKKTETQ and NBD-^{D}F^{D}F^{D}YGLKKTETQ were obtained by standard Fmoc solid-phase peptide synthesis. The pure peptides were obtained by reverse-phase high-performance liquid chromatography (HPLC). We first tested the self-assembly properties of both compounds. The negative-stained transmission electron microscopy (TEM) images indicated that both peptides could form nanofibers at the concentration of 500 μM (Figure S1, Supporting Information). They also possessed similar critical micelle concentration (CMC) values (0.24 and 0.16 mg/mL for NBD-FFYGLKKTETQ and NBD-^{D}F^{D}F^{D}YGLKKTETQ, respectively; Figure S2, Supporting Information). At higher concentrations, both compounds would form molecular hydrogels (Figure S3,Supporting Information). These observations suggested that they had similar self-assembly properties.

We then incubated mouse fibroblast NIH 3T3 cells with NBD-FFYGLKKTETQ and NBD-^{D}F^{D}F^{D}YGLKKTETQ at 500 μM each to investigate whether they could bind to actin or not. Surprisingly, the confocal fluorescence microscopy images showed a very different cellular distribution of both peptides. As shown in Figure 1, NBD-FFYGLKKTETQ distributed evenly in the whole cytoplasm of 3T3 cells (Figure 1A) but not colocalized with actin filaments. This observation suggested that the self-assembly property of the peptide would affect the actin binding ability of LKKTETQ and it was not an ideal candidate to image actin filaments. Surprisingly, we found that NBD-^{D}F^{D}F^{D}YGLKKTETQ preferentially localized on the cell membrane (Figure 1B) at 4 h, suggesting that D-amino acid might drive the membrane enrichment of the self-assembling peptide. Furthermore, we observed similar phenomenon in three other cell lines (in Figure 1, HepG2 cells in panels D and E; HeLa cells in panels G and H; and AD293 cells in panels J and K). These observations indicated that the membrane localization of NBD-^{D}F^{D}F^{D}YGLKKTETQ was not specific to a certain kind of cell line. We therefore switched our project to understand the phenomenon of different cellular distributions of self-assembling peptides.

To rule out the role of actin binding peptide LKKTETQ, we also synthesized NBD-^{D}F^{D}F^{D}YG^{D}L^{D}K^{D}K^{D}T^{D}E^{D}T^{D}Q with whole D-amino acids. NBD-^{D}F^{D}F^{D}YG^{D}L^{D}K^{D}K^{D}T^{D}E^{D}T^{D}Q had a similar self-assembly property to the aforementioned two peptides (Figures S1−S3, Supporting Information). The images in Figure 1C,F,I,L showed that the peptide with whole D-amino acids was also enriched on the membranes of 3T3, HepG2, HeLa, and AD293 cells, respectively. These observations suggested that peptides containing D-amino acids could be enriched on cell membranes. The MTT assay showed low cytotoxicities of the three peptides at 500 μM to 3T3, HepG2, HeLa, and AD293 cells, respectively (Figure S5, Supporting Information). The membrane localization of peptides with D-amino acids was quite stable. For instance, 3T3 cells treated with 500 μM of NBD-^{D}F^{D}F^{D}YGLKKTETQ also exhibited bright yellow fluorescence on their membranes at 12 h (Figure S6, Supporting Information).

We also studied the cellular distributions of the three peptides at a concentration (100 μM) lower than their CMC values. As shown in Figure S7, Supporting Information, the results indicated that three peptides mainly localized in the cytoplasma of both 3T3 and HeLa cells. These observations indicated that the peptides of NBD-^{D}F^{D}F^{D}YGLKKTETQ and NBD-^{D}F^{D}F^{D}YG^{D}L^{D}K^{D}K^{D}T^{D}E^{D}T^{D}Q could be enriched on cellular membranes only at their assembled stages. The results in Figure S8 (Supporting Information) indicated that the uptake of peptides were very different for the three peptides, and there were no correlations between cellular uptake and cellular distributions. We also changed the fluorescent aromatic capping group of NBD to Rhodamine B to produce Rho-

dx.doi.org/10.1021/am502250r | ACS Appl. Mater. Interfaces 2014, 6, 9815−9821

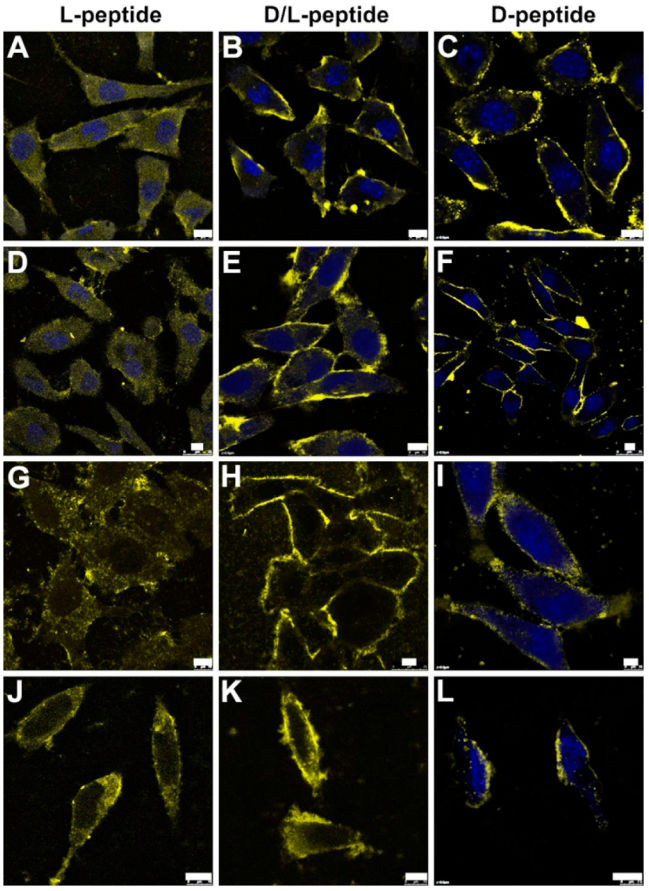

Figure 1. Confocal fluorescence images of (A–C) 3T3, (D–F) HepG2, (G–I) HeLa, and (J–L) AD293 cells incubated with 500 μM of (A, D, G, and J) NBD-FFYLKKTETQ, (B, E, H, and K) NBD-^{D}F^{D}F^{D}YLKKTETQ, and (C, F, I, and L) NBD-^{D}F^{D}F^{D}YG^{D}L^{D}K^{D}K^{D}T^{D}E^{D}T^{D}Q at 4 h. Scale bars in panels A–L represent 10 μm. Stock solution of peptide in PBS buffer (3 mM) at pH 7.4 was diluted by DMEM to give a final concentration of 500 μM.

FFYGLKKTETQ, Rho-^{D}F^{D}F^{D}YGLKKTETQ, and Rho-^{D}F^{D}F^{D}YG^{D}L^{D}K^{D}K^{D}T^{D}E^{D}T^{D}Q (Scheme S1, Supporting Information). The results in Figure S9 (Supporting Information) indicated that the three peptides distributed evenly in the cytoplasma of both 3T3 and HeLa cells at a concentration of 500 μM. Unlike NBD-capped peptides, Rho-capped ones possessed poor self-assembly properties, and they formed homogeneous solutions but not gels, even at a concentration of 1 wt % (5.3 mM; Figure S10, Supporting Information). These observations further demonstrated the necessity of self-assembled stage of the D-amino acid containing peptides to their membrane enrichments.

To test whether the membrane enrichment of D-peptides was ascribed from the LKKTETQ peptide sequence, we replaced the actin binding LKKTETQ peptide with a PDZ domain binding WRESAI peptide to afford NBD-FFYGWRESAI and NBD-^{D}F^{D}F^{D}YGWRESAI (Scheme 2). We also found that NBD-^{D}F^{D}F^{D}YGWRESAI was accumulated on the membranes of both 3T3 (Figure 2A) and HepG2 (Figure 2D) cells, while

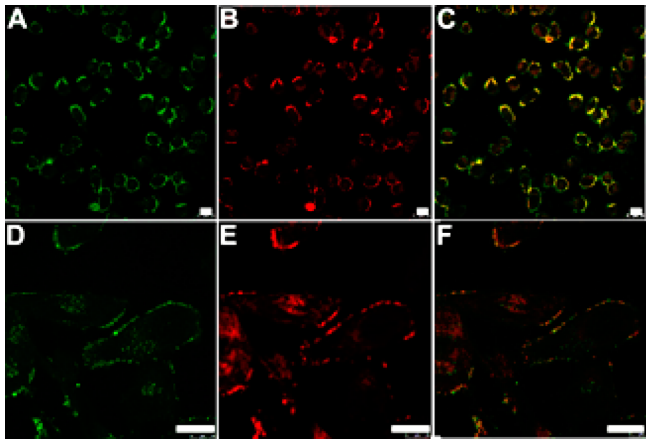

Figure 2. Co-localization of NBD-^{D}F^{D}F^{D}YGWRESAI and RBITC-Tip-1. Cells were incubated with peptide first for 4 h and then with RBITC-Tip-1 for 10 min. (A–C) 3T3 cells and (D and E) HepG2 cells. (A and D) NBD excitated at 488 nm, (B and E) Rhodamine B excitated at 561 nm, and (C and F) overlay images. Scale bars in panels A–F represent 15 μm. Stock solution of peptide in PBS buffer (3 mM) at pH 7.4 was diluted by DMEM to give a final concentration of 500 μM.

NBD-FFYGWRESAI was evenly distributed in the cytoplasm of both 3T3 (Figure S11A, Supporting Information) and HepG2 (Figure S11D, Supporting Information) cells at 4 h.

Scheme 2. Chemical Structures of NBD-FFYGWRESAI and NBD-^{D}F^{D}F^{D}YGWRESAI

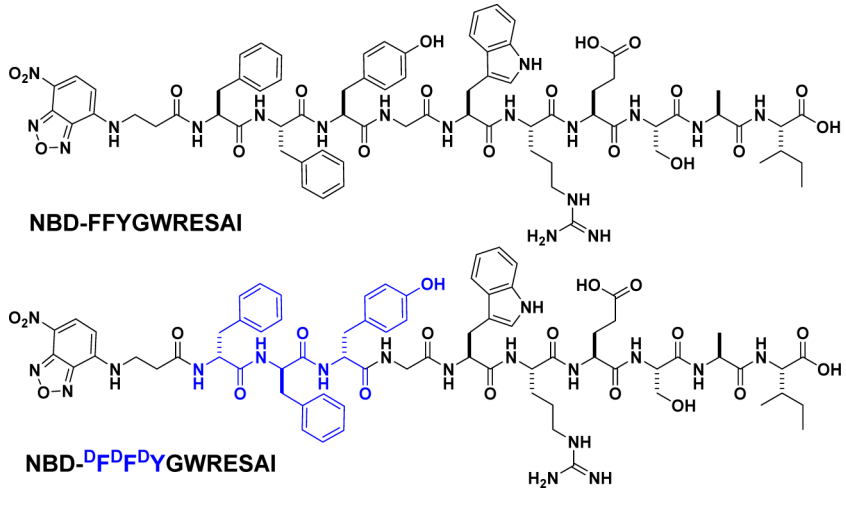

dx.doi.org/10.1021/am502250r | ACS Appl. Mater. Interfaces 2014, 6, 9815–9821

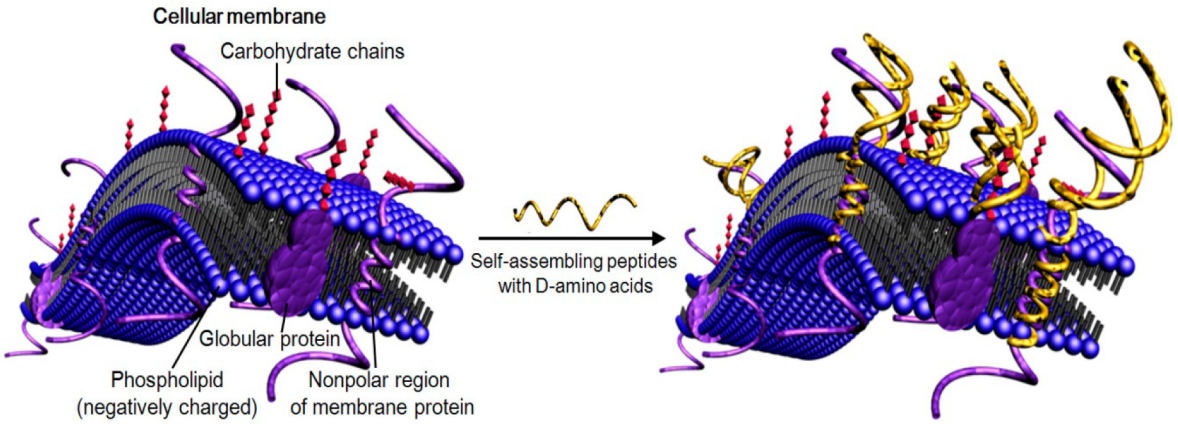

Figure 3. Schematic illustration of the proposed mechanism for the membrane enrichment of peptides containing D-amino acids.

These observations further demonstrated that the peptides containing D-amino acids would be enriched on cell membranes. This property of D-amino acid containing peptides suggested their great potential in cell surface engineering with functional peptides. What we needed to point out was that the membrane localization of NBD-^{D}F^{D}F^{D}YGWRESAI was not as stable as that of NBD-^{D}F^{D}F^{D}YGLKKTETQ, and we observed greater amounts of NBD-^{D}F^{D}F^{D}YGWRESAI in the cytoplasm of 3T3 cells at 12 h (Figure S12, Supporting Information).

Cell surface engineering was very important to camouflage cells or introduce functionalities to cells.[46−49] To demonstrate the membrane localization of peptides and the accessibility of WRESAI on cell membranea, we obtained a PDZ domain of tax-interacting protein-1 (Tip-1) by expression of it in *Escherichia coli* and labeled it with a Rhodamine B isothiocyanate (RBITC) to yield the RBITC-Tip-1 (Figure S13, Supporting Information). Tip-1 would bind to the hexapeptide WRESAI very tightly (K_d of about 6.5 nM).[50] It is noteworthy that free Tip-1 protein is difficult to penetrate into cells. We therefore could use the RBITC-Tip-1 to demonstrate the membrane localization and the accessibility of the hexapeptide of WRESAI. We pretreated 3T3 and HepG2 cells with NBD-^{D}F^{D}F^{D}YGWRESAI and incubated them with RBITC-Tip-1. As shown in Figure 2B,E, we observed bright red fluorescence from RBITC-Tip-1 on the membrane of both 3T3 and HepG2 cells pretreated with NBD-^{D}F^{D}F^{D}YGWRESAI. Additionally, the red fluorescence was colocalized well with the green fluorescence from NBD (Figure 2C,F). In comparison, upon the incubation of L-peptides (NBD-FFYGWRESAI) pretreated 3T3 and HepG2 cells with RBITC-Tip-1, respectively, we only observed green fluorescence from the L-peptides in cytoplasm and nearly no red fluorescence from the RBITC-Tip-1 (Figure S11, Supporting Information). These observations clearly demonstrated the membrane localization of NBD-^{D}F^{D}F^{D}YGWRESAI and the accessibility of WRESAI on the cell membrane. These observations also suggested that, by using NBD-^{D}F^{D}F^{D}YGWRESAI to first modify the cell surface and then treating with genetically engineered recombinant proteins based on Tip-1, we could introduce functional proteins to the cell surface.

We proposed a possible mechanism for the membrane enrichment of peptides containing D-amino acids (Figure 3). The conformations of peptides containing D-amino acids were nearly opposite to those of peptides containing only L-amino acids (Figure S14, Supporting Information). For example, the CD signal of NBD-^{D}F^{D}F^{D}YGLKKTETQ was almost opposite to that of NBD-FFYGLKKTETQ, while CD signals of NBD-^{D}F^{D}F^{D}YGLKKTETQ and NBD-^{D}F^{D}F^{D}YG^{D}L^{D}K^{D}K^{D}T-^{D}E^{D}T^{D}Q were similar (Figure S14, Supporting Information). Self-assembling L-peptides had been demonstrated to be able to form a 1:1 ratio complex with their D counterparts.[51] The nanofibers of peptides containing D-amino acids in our study might therefore interact with membrane proteins in a more stable way because proteins were consisted of only L-amino acids. Because the membrane localization of NBD-^{D}F^{D}F^{D}YGLKKTETQ was more stable than that of NBD-^{D}F^{D}F^{D}YGWRESAI and the former was more positively charged than the latter, we proposed that our peptides could also attach to negatively charged phospholipids by electrostatic interactions. These possible interactions might lead to the membrane enrichment of peptides containing D-amino acids. These possible interactions led to the membrane enrichment of peptides containing D-amino acids. However, the detailed mechanisms for membrane enrichment, cellular distribution of other peptides containing D-amino acids, and cellular distribution of peptides in other cell lines need to be investigated in future studies. There should be many factors that would affect the cellular distributions of peptides.

CONCLUSIONS

Recently, Xu and co-workers showed that D-peptides can selectively form supramolecular nanofibers and hydrogels at pericellular spaces, thus inhibiting cancer cells.[52] Stupp and co-workers developed smart supramolecular materials to instruct cell fates by varying the cohesive forces within nanofibers of supramolecular materials.[40] In this study, we found that self-assembling peptides containing D-amino acids can be enriched on cell membranes and demonstrated the possibility of using such D-amino acid-based peptides to engineer cell surfaces with functional peptides or proteins. These observations indicate that many factors will affect the cellular distributions of peptides, including the chirality of amino acids, conformation and sequence of the peptides, net charge of the peptide, and aromatic capping groups. We believe that we have provided a novel and versatile strategy to engineer cell surfaces, which will be very useful for cell therapy. Our study also highlighted the unusual property of D-peptides, which will stimulate the research interests to develop biomaterials of D-peptides for tissue engineering, drug delivery, and regenerative medicine. Our future studies will focus on the investigation of

mechanisms of cellular membrane enrichment of peptides containing D-amino acids and their applications in cell therapy.

EXPERIMENTAL SECTION

Materials. Fmoc-OSu and other Fmoc-amino acids were obtained from GL Biochem (Shanghai), Ltd. 2-Chlorotrityl chloride resin (1.0–1.2 mmol/g) was obtained from Nankai University Resin Co., Ltd. Chemical reagents and solvents were obtained from Alfa (China) and used as received. Paraformaldehyde was obtained from Beijing Solarbio Science & Technology Co., Ltd. Dulbecco's modified Eagle's medium (DMEM), fetal bovine serum (FBS), and penicillin/streptomycin were purchased from Gibco Corporation.

General Methods. Compounds were characterized by ^{1}H NMR (Bruker ARX-400) using DMSO-d_6 as the solvent. HPLC was conducted by a LUMTECH HPLC (Germany) system using a C_{18} RP column with MeOH (0.05% of TFA) and water (0.05% of TFA) as the eluents. LC–MS was performed by an LCMS-20AD (Shimadzu) system. HR-MS was obtained with the Agilent 6520 Q-TOF LC/MS using ESI-L low-concentration tuning mix (Lot No. LB60116 from Agilent Tech.).

Critical Micelle Concentration. The CMC values were determined by dynamic light scattering (DLS). Solutions containing different concentrations of peptides were first incubated in the tube for 12 h, 200 μL of each different concentration of compound was put into a cuvette, and the light scattering intensity was recorded for each concentration analyzed. DLS was performed on a laser light scattering spectrometer (BI-200SM) equipped with a digital correlator (BI-9000AT) at 532 nm at room temperature (22–25 °C).

Cell Culture. The 3T3, HepG2, HeLa, AD293 cells were maintained in our lab. Cells were cultured in DMEM supplemented with 10% v FBS and 100 U/mL penicillin/streptomycin at 37 °C in a humidified atmosphere of 5% CO_2.

Negative Staining for TEM Image. We followed these steps to prepare samples for TEM imaging:

(1) Sample solution was placed on the grid (3 μL, sufficient to cover the grid surface).

(2) Rinsing: about 10 s later, we placed a drop of the ddH_2O on parafilm, letting the grid touch the water drop, with the sample-loaded surface facing the parafilm. We tilted the grid and gently absorbed water from the edge of the grid using a filter paper sliver. (3 times)

(3) Staining (immediately after rinsing): we placed a large drop of the uranyl acetate (UA) staining solution on parafilm, letting the grid touch the stain solution drop, with the sample-loaded surface facing the parafilm. We tilted the grid and gently absorbed the stain solution from the edge of the grid using a filter paper sliver.

(4) We allowed the grid to air dry and examined the grid as soon as possible.

Cytotoxicity Evaluation of the Compounds. The cytotoxicity of different compounds was measured by MTT cell viability test. The cells were seeded in 96-well plates at a density of 5000 cells per well with a total medium volume of 100 μL and incubated for 24 h. Then, the solution was removed, and we added 100 μL of DMEM medium containing 500 μM compounds. Twenty-four hours later, we replaced the medium with fresh medium supplemented with 15 μL of MTT reagent (5 mg/mL). Four hours later, the medium containing MTT was removed, and DMSO (100 μL/well) was added to dissolve the formazan crystals. The optical density of the solution was measured at 490 nm using a microplate reader (Bio-RAD iMark, Hercules, CA). Cells without the treatment of the compounds were used as the control. The experiment was repeated three times.

Confocal Fluorescence Images. Different cells were first placed in 24-well plates (coverslips were first put into the well plates) at a density of 1×10^5 cells/mL and cultured in DMEM supplemented with 10% FBS, 100 U/ml penicillin, and 100 mg/mL streptomycin for 12 h to allow cell attachment. Then, the cells were washed three times with PBS buffer, and we added 500 μL of DMEM solution that contained 500 μM of compound. Four hours later, we removed the solution and washed three times with PBS buffer, fixed for 20 min in 4% PBS buffered paraformaldehyde, and then washed twice with PBS buffer, then put coverslip carefully on the glass slide. Cell imaging tests were conducted on Leica TSC SP8 Confocal Microscope. Images were captured with CFI VC 40× oil immersed optics.

Preparation of RBITC-Conjugated Tip-1. RBITC contains an ITC(—N═C═S) group, which is a reactive group commonly used to conjugate with the primary amines of proteins. First, Tip-1 (16 mg) was dissolved in pH 9 K_2CO_3 (2 mM, 30 mL) solution, where the target amine groups in Tip-1 were mainly unprotonated. We dissolved 3.5 mg of RBITC in 20 μL of anhydrous dimethyl sulfoxide (DMSO). A 10 μL of freshly prepared RBITC solution was added to the as-prepared Tip-1 solution to give a reaction ratio of 5 RBITC per each Tip-1. The mixture was shaken at 4 °C for 8 h. The unreacted RBITC was removed by dialysis. The products were measured by fluorescence spectroscopy and SDS-PAGE.

ASSOCIATED CONTENT

Supporting Information

TEM images and optical images of the gels, CMC values of all peptides, MTT assay, confocal images of cells treated with NBD-peptides at 100 μM and Rho-peptides at 500 μM, CD and fluorescence spectra, detailed synthetic procedures, and characterizations of compounds. This material is available free of charge via the Internet at http://pubs.acs.org.

AUTHOR INFORMATION

Corresponding Author

*E-mail: yangzm@nankai.edu.cn.

Author Contributions

The manuscript was written through contributions of all authors. All authors have given approval to the final version of the manuscript.

Notes

The authors declare no competing financial interest.

ACKNOWLEDGMENTS

We acknowledge the financial support from the NSFC (Grant Nos. 51222303, 51373079, and 81301311). We thank Professor Bing Xu at Brandeis University and Professor Yi Cao at Nanjing University for their valuable suggestions. We thank Professor Jiafu Long at Nankai University for protein expression.

REFERENCES

(1) Collier, J. H.; Rudra, J. S.; Gasiorowski, J. Z.; Jung, J. P. Multi-Component Extracellular Matrices based on Peptide Self-Assembly. *Chem. Soc. Rev.* **2010**, *39*, 3413–24.

(2) Ryan, D. M.; Nilsson, B. L. Self-Assembled Amino Acids and Dipeptides as Noncovalent Hydrogels for Tissue Engineering. *Polym. Chem.* **2012**, *3*, 18–33.

(3) Boekhoven, J.; Brizard, A. M.; Kowlgi, K. N.; Koper, G. J.; Eelkema, R.; Van Esch, J. H. Dissipative Self-Assembly of a Molecular Gelator by Using a Chemical Fuel. *Angew. Chem., Int. Ed.* **2010**, *49*, 4825–4828.

(4) Miao, X. M.; Cao, W.; Zheng, W. T.; Wang, J. Y.; Zhang, X. L.; Gao, J.; et al. Switchable Catalytic Activity: Selenium-Containing Peptides with Redox-Controllable Self-Assembly Properties. *Angew. Chem., Int. Ed.* **2013**, *52*, 7781–7785.

(5) Micklitsch, C. M.; Knerr, P. J.; MBranco, M. C.; Nagarkar, R.; Pochan, D. J.; Schneider, J. P. Zinc-Triggered Hydrogelation of a Self-Assembling β-Hairpin Peptide. *Angew. Chem., Int. Ed.* **2011**, *50*, 1577–1579.

(6) Nanda, J.; Biswas, A.; Adhikari, B.; Banerjee, A. A Gel-Based Trihybrid System Containing Nanofibers, Nanosheets, and Nanoparticles: Modulation of the Rheological Property and Catalysis. *Angew. Chem., Int. Ed.* **2013**, *52*, 5041–5045.

(7) Bowerman, C. J.; Nilsson, B. L. A Reductive Trigger for Peptide Self-Assembly and Hydrogelation. *J. Am. Chem. Soc.* **2010**, *132*, 9526−9527.
(8) Hirst, A. R.; Roy, S.; Arora, M.; Das, A. K.; Hodson, N.; Murray, P.; et al. Biocatalytic Induction of Supramolecular Order. *Nat. Chem.* **2010**, *2*, 1089−1094.
(9) Morris, K. L.; Chen, L.; Raeburn, J.; Sellick, O. R.; Cotanda, P.; Paul, A.; et al. Chemically Programmed Self-Sorting of Gelator Networks. *Nat. Commun.* **2013**, *4*, 1480.
(10) Sun, Z. F.; Li, G. Y.; He, Y. H.; Shen, R. J.; Deng, L.; Yang, M. H.; et al. Ferrocenoyl Phenylalanine: A New Strategy toward Supramolecular Hydrogels with Multistimuli Responsive Properties. *J. Am. Chem. Soc.* **2013**, *135*, 13379−13386.
(11) Jayawarna, V.; Ali, M.; Jowitt, T. A.; Miller, A. E.; Saiani, A.; Gough, J. E.; et al. Nanostructured Hydrogels for Three-Dimensional Cell culture through Self-Assembly of Fluorenylmethoxycarbonyl-Dipeptides. *Adv. Mater.* **2006**, *18*, 611−615.
(12) Zhou, M.; Smith, A. M.; Das, A. K.; Hodson, N. W.; Collins, R. F.; Ulijn, R. V.; et al. Self-Assembled Peptide-Based Hydrogels As Scaffolds for Anchorage-Dependent Cells. *Biomaterials* **2009**, *30*, 2523−2530.
(13) Jung, J. P.; Moyano, J. V.; Collier, J. H. Multifactorial Optimization of Endothelial Cell Growth Using Modular Synthetic Extracellular Matrices. *Integr. Biol.* **2011**, *3*, 185−96.
(14) Wang, H. M.; Wei, J.; Yang, C. B.; Zhao, H. Y.; Li, D. X.; Yin, Z. N.; et al. The Inhibition of Tumor Growth and Metastasis by Self-Assembled Nanofibers of Taxol. *Biomaterials* **2012**, *33*, 5848−5853.
(15) Webber, M. J.; Matson, J. B.; Tamboli, V. K.; Stupp, S. I. Controlled Release of Dexamethasone from Peptide Nanofiber Gels to Modulate Inflammatory Response. *Biomaterials* **2012**, *33* (28), 6823−6832.
(16) Zhao, F.; Ma, M. L.; Xu, B. Molecular Hydrogels of Therapeutic Agents. *Chem. Soc. Rev.* **2009**, *38*, 883−891.
(17) Cheetham, A. G.; Zhang, P.; Lin, Y. A.; Lock, L. L.; Cui, H. Supramolecular Nanostructures Formed by Anticancer Drug Assembly. *J. Am. Chem. Soc.* **2013**, *135*, 2907−2910.
(18) Gao, Y.; Kuang, Y.; Guo, Z. F.; Guo, Z. H.; Krauss, I. J.; Xu, B. Enzyme-Instructed Molecular Self-Assembly Confers Nanofibers and a Supramolecular Hydrogel of Taxol Derivative. *J. Am. Chem. Soc.* **2009**, *131*, 13576−13577.
(19) Soukasene, S.; Toft, D. J.; Moyer, T. J.; Lu, H.; Lee, H.-K.; Standley, S. M.; et al. Antitumor Activity of Peptide Amphiphile Nanofiber-Encapsulated Camptothecin. *ACS Nano* **2011**, *5*, 9113−9121.
(20) Lock, L. L.; Cheetham, A. G.; Zhang, P. C.; Cui, H. G. Design and Construction of Supramolecular Nanobeacons for Enzyme Detection. *ACS Nano* **2013**, *7*, 4924−4932.
(21) Bremmer, S. C.; Chen, J.; McNeil, A. J.; Soellner, M. B. A General Method for Detecting Protease Activity via Gelation and Its Application to Artificial Clotting. *Chem. Commun.* **2012**, *48*, 5482−5484.
(22) Ochi, R.; Kurotani, K.; Iked, M.; Kiyonaka, S.; Hamachi, I. Supramolecular Hydrogels Based on Bola-Amphiphilic Glycolipids Showing Color Change in Response to Glycosidases. *Chem. Commun.* **2013**, *49*, 2115−2117.
(23) Wada, A.; Tamaru, S.-i.; Ikeda, M.; Hamachi, I. MCM−Enzyme−Supramolecular Hydrogel Hybrid as a Fluorescence Sensing Material for Polyanions of Biological Significance. *J. Am. Chem. Soc.* **2009**, *131*, 5321−5330.
(24) Yamaguchi, S.; Yoshimura, L.; Kohira, T.; Tamaru, S.; Hamachi, I. Cooperation between Artificial Receptors and Supramolecular Hydrogels for Sensing and Discriminating Phosphate Derivatives. *J. Am. Chem. Soc.* **2005**, *127*, 11835−11841.
(25) Xu, X. D.; Lin, B. B.; Feng, J.; Wang, Y.; Cheng, S. X.; Zhang, X. Z.; et al. Biological Glucose Metabolism Regulated Peptide Self-Assembly as a Simple Visual Biosensor for Glucose Detection. *Macromol. Rapid Commun.* **2012**, *33*, 426−431.
(26) Gao, Y.; Shi, J.; Yuan, D.; Xu, B. Imaging Enzyme-Triggered Self-Assembly of Small Molecules Inside Live Cells. *Nat. Commun.* **2012**, *3*, 1033.
(27) Standley, S. M.; Toft, D. J.; Cheng, H.; Soukasene, S.; Chen, J.; Raja, S. M.; et al. Induction of Cancer Cell Death by Self-Assembling Nanostructures Incorporating a Cytotoxic Peptide. *Cancer Res.* **2010**, *70*, 3020−3026.
(28) Sinthuvanich, C.; Veiga, A. S.; Gupta, K.; Gaspar, D.; Blumenthal, R.; Schneider, J. P. Anticancer β-Hairpin Peptides: Membrane-Induced Folding Triggers Activity. *J. Am. Chem. Soc.* **2012**, *134*, 6210−6217.
(29) Kuang, Y.; Xu, B. Disruption of the Dynamics of Microtubules and Selective Inhibition of Glioblastoma Cells by Nanofibers of Small Hydrophobic Molecules. *Angew. Chem., Int. Ed.* **2013**, *52*, 6944−6948.
(30) Rudra, J. S.; Sun, T.; Bird, K. C.; Daniels, M. D.; Gasiorowski, J. Z.; Chong, A. S.; et al. Modulating Adaptive Immune Responses to Peptide Self-Assemblies. *ACS Nano* **2012**, *6*, 1557−1564.
(31) Rudra, J. S.; Mishra, S.; Chong, A. S.; Mitchell, R. A.; Nardin, E. H.; Nussenzweig, V.; et al. Self-Assembled Peptide Nanofibers Raising Durable Antibody Responses against a Malaria Epitope. *Biomaterials* **2012**, *33*, 6476−6484.
(32) Silva, G. A.; Czeisler, C.; Niece, K. L.; Beniash, E.; Harrington, D. A.; Kessler, J. A.; et al. Selective Differentiation of Neural Progenitor Cells by High-Epitope Density Nanofibers. *Science* **2004**, *303*, 1352−1355.
(33) Liang, G. L.; Yang, Z. M.; Zhang, R. J.; Li, L. H.; Fan, Y. J.; Kuang, Y.; et al. Supramolecular Hydrogel of a D-Amino Acid Dipeptide for Controlled Drug Release in Vivo. *Langmuir* **2009**, *25*, 8419−8422.
(34) Li, J. Y.; Gao, Y.; Kuang, Y.; Shi, J. F.; Du, X. W.; Zhou, J.; et al. Dephosphorylation of D-Peptide Derivatives to Form Biofunctional, Supramolecular Nanofibers/Hydrogels and Their Potential Applications for Intracellular Imaging and Intratumoral Chemotherapy. *J. Am. Chem. Soc.* **2013**, *135*, 9907−9914.
(35) Luo, Z. L.; Zhao, X. J.; Zhang, S. G. Structural Dynamic of a Self-Assembling Peptide d-EAK16 Made of Only D-Amino Acids. *PLoS One* **2008**, *3*, e2364.
(36) Li, J.; Kuang, Y.; Gao, Y.; Du, X.; Shi, J.; Xu, B. D-Amino Acids Boost the Selectivity and Confer Supramolecular Hydrogels of a Nonsteroidal Anti-Inflammatory Drug (NSAID). *J. Am. Chem. Soc.* **2013**, *135*, 542−545.
(37) Kuang, Y.; Yuan, D.; Zhang, Y.; Kao, A.; Du, X. W.; Xu, B. Interactions between Cellular Proteins and Morphologically Different Nanoscale Aggregates of Small Molecules. *RSC Adv.* **2013**, *3*, 7704−7707.
(38) Kuang, Y.; Xu, B. Nanofibers of Small Hydrophobic Molecules Disrupt Dynamics of Microtubles and Selectively Inhibit Gliobalstoma Cells. *Angew. Chem., Int. Ed.* **2013**, *52*, 6944−6948.
(39) Yang, Z. M.; Xu, K. M.; Guo, Z. F.; Guo, Z. H.; Xu, B. Intracellular Enzymatic Formation of Nanofibers Results in Hydrogelation and Regulated Cell Death. *Adv. Mater.* **2007**, *17*, 3152−3156.
(40) Newcomb, C. J.; Sur, S.; Orton, J. H.; Lee, O. S.; Matson, J. B.; Boekhoven, J.; Yu, J. M.; Schatz, G. C.; Stupp, S. I. Cell Death versus Cell Survival Instructed by Supramolecular Cohesion of Nanostructures. *Nat. Commun.* **2014**, *5*, 3321.
(41) Mahler, A.; Reches, M.; Rechter, M.; Cohen, S.; Gazit, E. Rigid, Self-Assembled Hydrogel Composed of a Modified Aromatic Dipeptide. *Adv. Mater.* **2006**, *18*, 1365−1368.
(42) Zheng, W.; Gao, J.; Song, L.; Chen, C.; Guan, D.; Wang, Z.; et al. Surface-Induced Hydrogelation Inhibits Platelet Aggregation. *J. Am. Chem. Soc.* **2013**, *135*, 266−271.
(43) Zhuang, Y. D.; Chiang, P. Y.; Wang, C. W.; Tan, K. T. Environment-Sensitive Fluorescent Turn-On Probes Targeting Hydrophobic Ligand-Binding Domains for Selective Protein Detection. *Angew. Chem., Int. Ed.* **2013**, *52*, 8124−8128.
(44) Cai, Y. B.; Wang, H. M.; Ding, D.; Wang, L.; Yang, Z. M. Environment-Sensitive Fluorescent Supramolecular Nanofibers for Imaging Applications. *Anal. Chem.* **2014**, *86*, 2193−2199.

(45) Philp, D.; Badamchian, M.; Scheremet, B.; Nguyen, M.; Goldstein, A. L.; Kleinman, H. K. Thymosin Beta(4) and a Synthetic Peptide Containing Its Actin-Binding Domain Promote Dermal Wound Repair in Db/Db Diabetic Mice and in Aged Mice. *Wound Repair Regen.* **2003**, *11*, 19−24.
(46) Wilson, J. T.; Cui, W. X.; Kozovskaya, V.; Kharlampieva, E.; Pan, D.; Qu, Z.; et al. Cell Surface Engineering with Polyelectrolyte Multilayer Thin Films. *J. Am. Chem. Soc.* **2011**, *133*, 7054−64.
(47) Stephan, M. T.; Irvine, D. J. Enhancing Cell Therapies from the Outside In: Cell Surface Engineering Using Synthetic Nanomaterials. *Nano Today.* **2011**, *6*, 309−325.
(48) Jeong, J. H.; Schmidt, J. J.; Kohman, R. E.; Zill, A. T.; DeVolder, R. J.; Smith, C. E.; et al. Leukocyte-Mimicking Stem Cell Delivery via in Situ Coating of Cells with a Bioactive Hyperbranched Polyglycerol. *J. Am. Chem. Soc.* **2013**, *135*, 8770−8773.
(49) Peng, Y. J.; Kim, D. H.; Jones, T. M.; Ruiz, D. I.; Lerner, R. A. Engineering Cell Surfaces for Orthogonal Selectability. *Angew. Chem., Int. Ed.* **2013**, *52*, 336−340.
(50) Zhang, X. L.; Chu, X. L.; Wang, L.; Wang, H. M.; Liang, G. L.; Zhang, J. X.; et al. Rational Design of a Tetrameric Protein to Enhance Interactions between Self-Assembled Fibers Gives Molecular Hydrogels. *Angew. Chem., Int. Ed.* **2012**, *51*, 4388−4392.
(51) Swanekamp, R. J.; Dimaio, J. T. M.; Bowerman, C. J.; Nilsson, B. L. Coassembly of Enantiomeric Amphipathic Peptides into Amyloid-Inspired Rippled Beta-Sheet Fibrils. *J. Am. Chem. Soc.* **2012**, *134*, 5556−5559.
(52) Kuang, Y.; Shi, J. F.; Li, J.; Yuan, D.; Alberti, K. A.; Xu, Q. B.; Xu, B. Pericellular Hydrogel/Nanonets Inhibit Cancer Cells. *Angew. Chem., Int. Ed.* **2014**, *53*, 1−6.